processes

MDPI

Article

Catalytic Activity of Ni Nanotubes Covered with Nanostructured Gold

Alena Shumskaya [1], Larissa Panina [2,3,*], Alexander Rogachev [1], Zhanna Ihnatovich [1], Artem Kozlovskiy [4,5], Maxim Zdorovets [4,5,6], Egor Kaniukov [2,6,7] and Ilya Korolkov [4,5]

1 Institute of Chemistry of New Materials of the National Academy of Sciences of Belarus, 220004 Minsk, Belarus; lunka7@mail.ru (A.S.); Rogachev78@mail.ru (A.R.); ignatovichz@inbox.ru (Z.I.)
2 National University of Science and Technology MISiS, 101000 Moscow, Russia; ka.egor@mail.ru
3 Institute of Physics, Mathematics and Information Technology, Immanuel Kant Baltic Federal University, 236001 Kaliningrad, Russia
4 Engineering Department, L.N. Gumilyov Eurasian National University, Astana 010000, Kazakhstan; artem88sddt@mail.ru (A.K.); Mzdorovets@gmail.com (M.Z.); korolkovelf@gmail.com (I.K.)
5 The Institute of Nuclear Physics, Almaty 050000, Kazakhstan
6 Institute of New Materials and Technologies, Ural Federal University named after B.N.Yeltsin, 620000 Ekaterinburg, Russia
7 Laboratory of Single Crystal Ggrowth, South Ural State University, 454000 Chelyabinsk, Russia
* Correspondence: drlpanina@gmail.com

Abstract: Ni nanotubes (NTs) were produced by the template method in the pores of ion-track membranes and then were successfully functionalized with gold nanoparticles (Ni@Au NTs) using electroless wet-chemical deposition with the aim to demonstrate their high catalytic activity. The fabricated NTs were characterized using a variety of techniques in order to determine their morphology and dimensions, crystalline structure, and magnetic properties. The morphology of Au coating depended on the concentration of gold chloride aqueous solution used for Au deposition. The catalytic activity was evaluated by a model reaction of the reduction of 4-nitrophenol by borohydride ions in the presence of Ni and Ni@Au NTs. The reaction was monitored spectrophotometrically in real time by detecting the decrease in the absorption peaks. It was found that gold coating with needle-like structure formed at a higher Au-ions concentration had the strongest catalytic effect, while bare Ni NTs had little effect. The presence of a magnetic core allowed the extraction of the catalyst with the help of a magnetic field for reusable applications.

Keywords: template synthesis; magnetic nanotubes; Ni@Au nanocomposite; Au nanocatalysts1

Citation: Shumskaya, A.; Panina, L.; Rogachev, A.; Ihnatovich, Z.; Kozlovskiy, A.; Zdorovets, M.; Kaniukov, E.; Korolkov, I. Catalytic Activity of Ni Nanotubes Covered with Nanostructured Gold. *Processes* **2021**, *9*, 2279. https://doi.org/10.3390/pr9122279

Academic Editor: Sergei Alexandrov

Received: 23 November 2021
Accepted: 14 December 2021
Published: 20 December 2021

1. Introduction

Gold nanostructures have a number of specific properties, including high conductivity, localized plasmon resonance, and biocompatibility, which explains their wide use in various fields from sensing and imaging to photothermal therapy [1]. Owing to high surface energy and large surface area, Au nanoparticles, in contrast with bulk gold, are considered a key catalyst in various reactions, providing high activity and selectivity [2,3]. In many cases, the Au–nano catalytic activity remains very high even in the absence of solvents and without use of harsh conditions (strong oxidants, high temperatures, and pressures). The catalytic efficiency of nanostructured gold depends on a number of factors such as particle size and shape [4–6]. Typically, smaller Au particles behave better due to a larger number of surface atoms. The shape may also influence the number of surface atoms and affinity. Therefore, controlled morphology of Au nanoparticles is important for catalytic applications [7–9].

Another factor affecting catalytic efficiency is the support on which the particles are evenly distributed and therefore exposed to more reagents. Thus, carbon nanotubes are promising as a catalyst support for metal nanoparticles [10,11]. The support can have magnetic properties, which makes it possible to control the catalyst by an external

magnetic field, simplifying many processes such as stirring during the reaction, recovery, or purification of the catalyst [12]. In this work, hollow nickel nanotubes (NTs) synthesized by a template method and then coated with a stable layer of nanostructured gold were proposed as catalysts and tested using a model reaction of the reduction of 4-nitrophenol (4-NP) [13]. In general, 1D-nanomaterials such as NTs have potential for applications in catalysis [14].

Among the noble metallic nanostructures, Ag and Cu are also attractive in catalysis owing to their lower cost and high reactivity and selectivity. In particular, the reduction in p-NP by borohydride with the assistance of Ag nanoparticles was accepted as an alternative route to effectively produce p-aminophenol (p-AP) [15,16]. However, the catalytic activity of AgNPs is not as good as AuNPs. Depending on the reaction type, bimetallic Au nanomaterials such as AuPd could be more preferred [17,18].

Most of the research is devoted to the search for stabilization of gold nanoparticles and their immobilization on various substrates to improve their catalytic activity, stability, and durability. Standard procedures for creation of a gold shell around metal nanoparticles are based on a two-step process: first, an inner metal core is synthesized using inorganic salts of Me^{n+} (for a magnetic core, Me = Fe, Ni, Co), and then the shell is formed by successive reduction of Au in the presence of sodium citrate or sodium borohydride [19–21]. In another approach, an Au layer is produced by deposition through an additional polymer or silica compound layer [20]. Additionally, the template electrochemical synthesis can be employed where the matrix with deposited Au tubes is used as a template for inner metal deposition [22–24]. The developed methods make it possible to produce a gold coating with a predefined thickness and with various morphologies, such as flat layers and individual particles in the form of ellipsoidal granules, hemispheres, and needles.

The study of cost-effective methods for the production of stable, easily controllable, and reusable catalysts remains an important challenge in the field of catalysis research. Nanomaterials structured as 'magnetic core-Au shell' can be good candidates in the field of efficient and environmentally friendly catalysts. The possible control of the catalyst by an external magnetic field simplifies many processes such as stirring during the reaction, recovery, or purification of the catalyst. In such systems, iron oxide nanoparticles are most frequently used as a magnetic core [12,20,25]. Replacing them with 3D metals brings stronger ferromagnetic properties. In particular, Ni, as naturally occurring transition material, can be more advantageous as a magnetic core. Furthermore, elongated magnetic nanostructures in the form of nanowires and NTs should outperform the spherical magnetic beads in catalytic applications [26].

The proposed bimetallic nanostructures of the type nickel core-Au shell (Ni@Au) represent a catalytic system for several types of reactions, such as hydrodechlorination of 2,4-dichlorophenol [12] and chlorobenzene [27], chemoselective hydrogenation of nitroarenes [28], selective hydrogenation of alkynes or dienes and levulinic acid [29], methanation of synthesis gas [30], and light hydrocarbons reforming [31]. Gold-on-magnetic metal catalyst can be used in oxidation processes: both complete oxidations, used to catalytically destroy various toxic compounds, and selective oxidation, used for organic synthesis in fine chemistry to get the desired products such as oxidative decomposition of volatile organic compounds, selective oxidation of alcohols, hydrocarbons, and sugars.

Here, we study the reduction of 4-NP by $NaBH_4$ in the presence of Ni@Au NTs, which is regarded as a 'model catalytic reaction'. This implies that the reaction yields a single product, and it does not proceed in the absence of a catalyst. On the other hand, the reduction of nitro derivatives is very important due to their pollutant nature [13]. The reaction was monitored by UV–vis spectroscopy by the decrease in the absorption peak of 4-NP at 400 nm. Ascribing this decrease to the concentration of 4-NP, the reaction rate was determined, and its change was used to compare the performances of Ni@Au NTs as catalysts.

2. Materials and Methods

A two-stage process was used to produce Ni@Au NTs: Ni NTs were synthesized in the pores of ion-track matrices by the method of template synthesis, and then gold was deposited on the surface of the NTs by wet chemistry.

Track-etched membranes with a thickness of 12 μm (pore diameter of 380 ± 20 nm, density of 4×10^7 cm^{-2}) based on polyethylene terephthalate (PET) were used as templates. Manufacturing and control parameters of PET membranes were demonstrated in previous works [32–36]. In short, PET films (Mitsubishi Polyester Film, Germany) were irradiated by Kr-ions with an energy of 1.75 MeV/nucleon and an ion fluence of 4×10^7 ions/cm^2 using a DC-60 accelerator (available in Astana branch of the Institute of Nuclear Physics of Kazakhstan). After chemical treatment in 2.2 M NaOH at 85 °C, membranes of a given diameter were obtained.

Electrochemical deposition was carried out at a potential difference of 1.75 V (negative potential) in a two-electrode electrochemical cell using an aqueous solution of $NiSO_4 \times 6H_2O$ (100 g/L) and H_3BO_3 (45 g/L) at room temperature [37,38]. The process was controlled by a chronoamperometric method of measuring the voltage vs. time characteristic with an Agilent 34,410 system. Before electrochemical deposition, a thin layer of gold (10 nm) was magnetron sputtered on one side of the membrane. The resulting tubes length was 8.8 ± 0.2 μm, so they were shorter than the thickness of the PET template to prevent the formation of NTs overlaps. The external diameters corresponded to the pore diameters. The internal diameters were 220 ± 20 nm, and the wall thickness was approximately equal to 80 nm.

After the synthesis of nanotubes, the PET template was etched in a 5 M NaOH solution for 4 h and at a temperature of 85 °C until the template was completely evacuated.

The electroless wet-chemical method was used to coat NTs with gold. The deposition was carried out from the aqueous solution of the gold chloride with two concentrations of 0.005 M and 0.01 M and 1%-hydrofluoric acid [39] at 25 °C for 30 s. After gold deposition, the samples were washed with NaOH (1%) to neutralize hydrofluoric acid, water, and ethanol. This process involves the replacement of the Ni atoms on the NTs surface with Au atoms through a reduction–oxidation reaction. The sequence of reactions leading to the formation of a nanostructured gold coating on the surface of Ni NTs is represented by Equations (1)–(4):

$$3Ni^0 + 2Au^{3+} \rightarrow 2Au^0 + 3Ni^{2+} \quad (1)$$

$$Au^{3+} \xrightarrow{e^-} Au^{2+} \xrightarrow{e^-} Au^{+} \xrightarrow{e^-} Au^0, \quad (2)$$

$$2Au^{2+} \rightarrow Au^{3+} + Au^{+}, \quad (3)$$

$$nAu^0 \rightarrow Au_n^0\ (NSs). \quad (4)$$

The fabricated NTs were characterized using a variety of techniques in order to determine their morphology and dimensions, crystalline structure, magnetic, and optical properties. Structural features were examined using scanning electron microscopy (SEM, Hitachi TM3030), scanning transmission electron microscopy (STEM, Hitachi SU9000) at simultaneous bright-field and annular dark-field imaging regimes, transmission electron microscopy (TEM, JEOL JEM-100). Energy dispersive X-Ray analysis (EDX, JED-2300 Analysis Station at JEOL JCM-6000 Plus Neoscope microscope) and X-ray diffraction analysis (XRD, Bruker D8 ADVANCE, Cu K_α radiation) were used for elemental and crystallographic characterization.

The basic magnetic parameters were determined from the hysteresis loops measured with the help of vibrating sample magnetometer (universal measuring system "Liquid Helium Free High Field Measurement System, Cryogenic LTD, London, UK"). The magnetizing field was up to ±1 T. The measurements were taken at room temperature. The samples were prepared in the form of powders.

The catalytic activity of nanotubes was examined using a model reaction of the reduction of 4-nitrophenol (4-NP) by borohydride ions in the aqueous solution. For

catalytic reduction of 4-NP, sodium borohydride solution (0.5 mL, 0.1 mM) was added to 4-NP (4.5 mL, 0.11 mM) contained in a glass vessel. After that, a predetermined amount of Ni@Au NTs was added, and immediately, UV/Vis spectra of the sample were taken every 2 min in the wavelength range of 200–600 nm. Fourier-transform infrared (FTIR) spectrometer (InfraLUM FT-08) was used to record FTIR spectra (range 400–4000 cm^{-1}, 25 scans, 2 cm^{-1} resolution, on ATR accessory (PIKE, PIKE Technologies, Madison, USA)).

After the reaction, the catalysts were removed using a magnet, washed three times with ethanol and distilled water, and freeze-dried for reuse in the next run.

3. Results and Discussion

The determination of the elemental composition by the EDX method confirmed that the originally produced NTs by the electrochemical deposition consisted of pure nickel, and they were free from any impurities. The SEM image of Ni NTs shown in Figure 1a demonstrates their smooth surface and a hollow structure. Similar results were previously obtained in [37,38].The XRD pattern given in Figure 1b shows that Ni NTs have a (111) preferred direction of growth, as this peak is much larger compared to the other peaks. The XRD pattern recorded at diffraction angles of $20 < 2\theta < 35°$ contained the halo typical of PET films [36]. The crystal structure was a face centered cubic (fcc) with the lattice parameter $a = 3.5176 \pm 0.0007$ Å and an average crystallite size of 17.5 ± 1.1 nm. The XRD analysis confirmed pure structure of Ni NTs (phase concentration of Ni is 100%) with a degree of crystallinity of 78%, which is associated with a well-formed crystal lattice, as well as a low content of disordering regions. Structural parameters of initial Ni NTs are collected in Table 1.

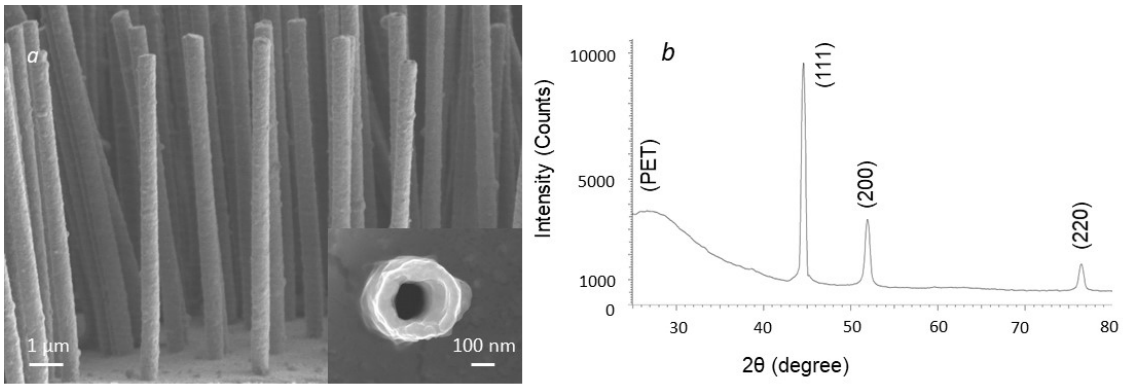

Figure 1. SEM image in (**a**) and XRD pattern in (**b**) of an array of Ni NTs in PET template. Similar results were previously obtained in [37,38].

Table 1. Structural parameters of Ni NTs.

Phase	(hkl)	2θ°	d, Å	Crystallite Size, nm	Lattice Parameter, Å	FWHM
Ni-Cubic Fm-3m(225)	111	44.586	2.03015	17.35	3.51760	0.550
	200	51.835	1.76354	15.68		0.629
	220	76.601	1.24424	17.67		0.636

After the synthesis of nanotubes, the PET template was completely etched. The deposition of gold on the surface of nickel nanotubes carried out by the wet chemistry method with two different concentrations of gold salt in the solution (0.005 M and 0.01 M) resulted in different coatings. The analysis of SEM images (Figure 2) showed that gold covers Ni NTs surface in different manner, depending on the concentration of gold ions in the solutions. Previous results on structural and optical properties of Ni NTs plated with Au for use as SERS substrates (surface enhanced Raman scattering) were reported in [39].

With increase in the concentration, the surface morphology of the gold layer changes. At a concentration of 0.005 M, a thin gold film is formed having a granular structure with a grain size of less than 50 nm. At a concentration of 0.01 M, gold nanostructures grow on the surface of NTs in the form of needles up to 200–250 nm in length.

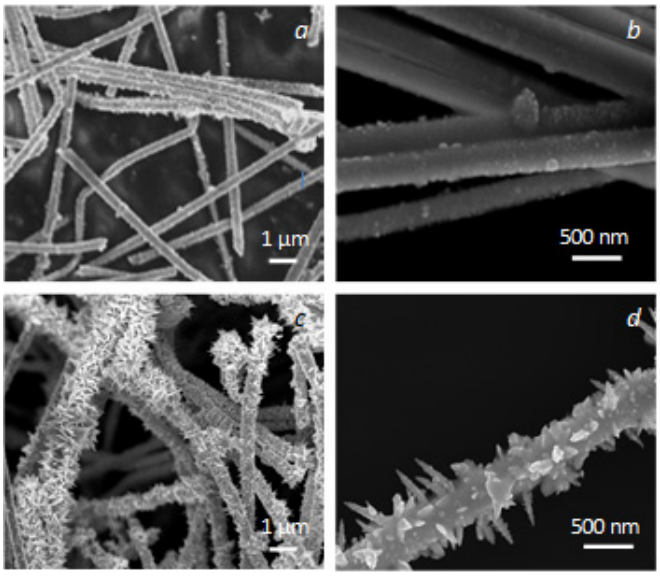

Figure 2. SEM images of Ni@Au NTs: (**a**,**c**)—prepared with gold chloride concentrations of 0.005 M and 0.01 M, respectively. (**b**,**d**)—the corresponding enlarged patterns.

To determine the gold content in the composition of coated nanotube samples, EDX analysis was performed. The EDX mapping shown in Figure 3 simultaneously records nickel and gold and their quantities.

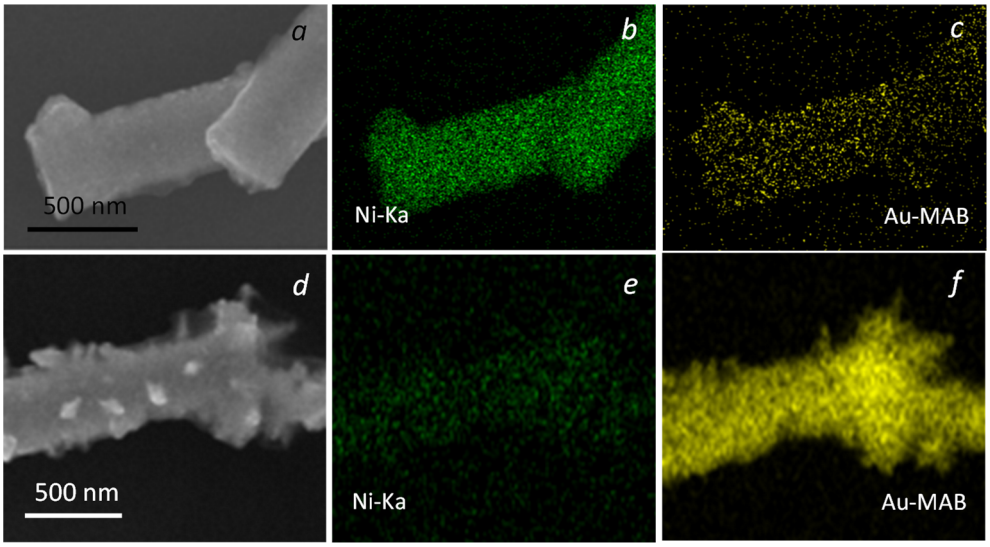

Figure 3. SEM image (**a**,**d**), nickel and gold mapping (**b**,**c**,**e**,**f**) for Ni@Au NTs prepared with different concentration of Au 0.005 M (**a**–**c**) and 0.01 M (**d**–**f**), respectively. The images for 0.01 M concentration are similar to those published in [39].

The results of EDX showed that the atomic ratio of Au and Ni in the structure was 21% and 79% for samples produced with a gold chloride concentration of 0.005 M, and this percentage changed to 68% and 32% when the gold chloride concentrations increased to 0.01 M, respectively. The spectra showed that the surface of the nanotubes was uniformly covered with gold, and the needle-like nanostructures are entirely composed of gold.

The XRD spectra of Ni@Au NTs shown in Figure 4 reveal the presence of phases of Ni and Au. In the XRD patterns of the samples with two gold chloride concentrations, low-intensity peaks correspond to 0.005 M, and higher intensity peaks are for samples with 0.01 M. The fcc phases of Ni and Au are identified in both cases. Structural parameters of Ni@Au NTs are presented in Table 2. The crystallographic parameters were calculated from the main peaks of Au (111) and Ni (111). For Ni, the unit lattice parameter and crystallites size slightly increased, probably due to the aching process of the Ni surface during the reaction. The position of the Au (200) peak close to the Ni (111) peak may also result in apparent increase in the peak widths. For Au, the lattice parameter *a* slightly increases from 4.0618 Å to 4.08243 Å with the increase in concentration. The phase concentration of gold increases from 20.5% to 38.9% with the increase in concentration of Au ions in the solution. This differs from the results obtained with the EDX method, which predominantly reflects the concentrations in the surface layer and often does not reliably determine the volume or mass content of components. On the other hand, XRD is an accurate method for determining the phase composition of a crystalline material. Equations (1)–(4) show the sequential reduction of gold to a metallic state. Therefore, the large difference in the relative mass concentration of gold in the composite can be explained by both the specificity of the methods used and by the phase state of gold (the presence of a non-metallic phase) on the surface of nickel nanotubes. The presence of mixed phases such as substitutional or interstitial solutions was not detected. A slight increase in the degree of crystallinity is due to the formation of the fcc-Au phase.

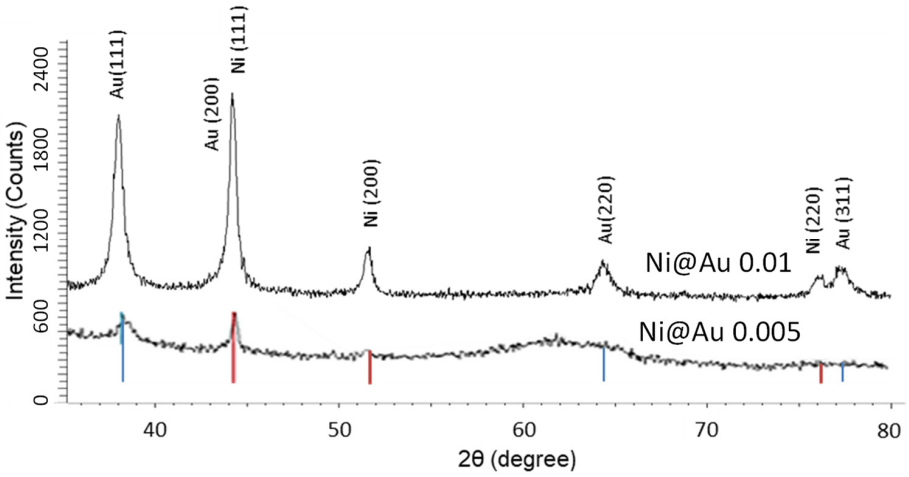

Figure 4. XRD of Ni@Au NTs with two concentrations of 0.005 M (bottom curve) and 0.01 M (upper curve). The lower intensity peaks are due to smaller amount of NTs used for the investigation.

Table 2. Structural parameters of Ni@Au nanotubes.

Ni@Au NTs, Concentration of Au in Solution	Phase	Crystallites Size, nm	Lattice Parameter, Å	Phase Concentration, %
0.005 M	Ni-Cubic Fm-3m(225)	19.87 ± 2.01	3.51991	79.5
	Au-cubic Fm-3m(225)	12.29 ± 1.15	4.0618	20.5
0.01 M	Ni-Cubic, Fm-3m(225)	21.08 ± 1.61	3.53442	61.1
	Au-Cubic, Fm-3m(225)	16.6 ± 1.35	4.08243	38.9

The hysteresis loops of Ni and Ni@Au NTs powder samples are shown in Figure 5. The loops are typical for ferromagnetic materials and correspond to previously obtained results for Ni NTs [38]. The magnetic properties: coercivity and squatness of hysteresis loops for samples of Ni and Ni@Au NTs are slightly different. Thus, the coercivity increases from 75 Oe for Ni NTs to 82 Oe for Ni@Au NTs (0.005 M) and to 87 Oe for Ni@Au NTs (0.01 M). The remanence to saturation value of about 0.315 is almost the same for all the samples. A change in magnetic properties of magnetic nanomaterials coated with functional layers is often observed, which is associated with surface effects, such as fixation of the magnetic moment due to the coating and a change in the interaction between particles [40]. In our case, the change was insignificant.

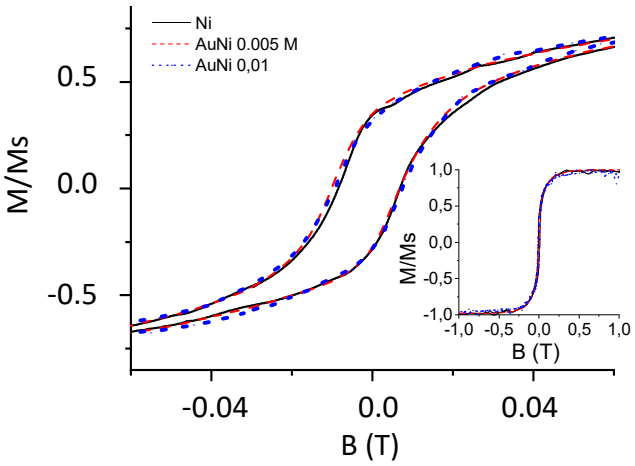

Figure 5. Hysteresis loops of Ni, Ni@Au (0.005), and Ni@Au (0.01) NTs. All the samples for measurements were prepared in the form of powders. Insert shows the magnetization in larger fields saturating the samples.

To demonstrate the catalytic activity, the reaction of reduction of 4-nitrophenol by borohydride ions in aqueous solution was used, which meets the following requirements:

i. A simple and well-controlled chemical reaction of the transformation of substance A into B should be observed in the presence of nanostructures, and the termination of the reaction without them;
ii. Analysis of reaction kinetics must be performed by simple and accurate methods (e.g., UV–Vis spectroscopy), and the reaction mechanism, including a possible intermediate state, must be precisely known;
iii. The reaction must proceed under rather mild conditions in order to avoid any side reactions or possible dissolution of the nanoparticle.

To understand the efficiency of the catalysts, as well as the possible influence of the nickel core on the catalytic activity, the reaction was monitored spectrophotometrically in the presence of the following samples: Ni NTs, 'nickel core-gold shell' NTs of two different morphology of the gold coating, and accordingly, the amount of gold. 4-nitrophenol has a characteristic absorption peak at about 400 nm, which remains almost unchanged in the presence of Ni NTs, as shown in Figure 6b. The absorption peak decreases in the presence of Ni@Au (0.005) NTs (Figure 6c) and almost disappears after 10 min of addition of Ni@Au (0.01) NTs, which indicates almost complete conversion of 4-nitrophenol to 4-aminophenol. Simultaneously, a peak at around 299 nm corresponding to 4-aminophenol appears which evidences the reaction (indicated in Figure 6 by arrow). Therefore, under the experimental conditions, the considered reduction reaction was not possible without the use of gold nanoparticles of sufficient amount and specific morphology. The concentration

of remaining p-nitrophenol C_{nit} as a function of time can be described by introducing the apparent rate constant (k_{app}) [13,16,41]:

$$\frac{dC_{nit}}{dt} = -k_{app}C_{nit} \tag{5}$$

Considering that the absorption peak intensity is proportional to C_{nit}, the following relationship is held:

$$k_{app}t = \ln A(t)/A_0, \tag{6}$$

where A_0 corresponds to the absorption intensity of p-nitrophenolate ions at 400 nm, and $A(t)$ corresponds to the measured absorption peak at time t. This allows us to use a linear fit with respect to time of the function $\ln A(t)/A_0$ as an indicator of the catalytic activity of different samples.

The largest value of k_{app} of 1.7×10^{-3} s^{-1} is obtained in the presence of Ni@Au NTs (0.01). This parameter reduces to 0.532×10^{-3} s^{-1} when Ni@Au NTs (0.005) are used, and down to 0.19×10^{-3} s^{-1} in the presence of Ni NTs. It is seen that Ni NTs on their own are not a catalyst.

The obtained results for the reaction rate k_{app} can be compared with the use of other Au nanostructures. Depending on the size, shape, and surrounding ligands, this value may range from 0.8×10^{-3} s^{-1} up to 7.2–7.9 $\times 10^{-3}$ s^{-1} [6,23,41,42]. Therefore, we achieved a moderate value of k_{app} but the technology has a potential of further optimization, since an improved performance with changes in Au morphology was demonstrated.

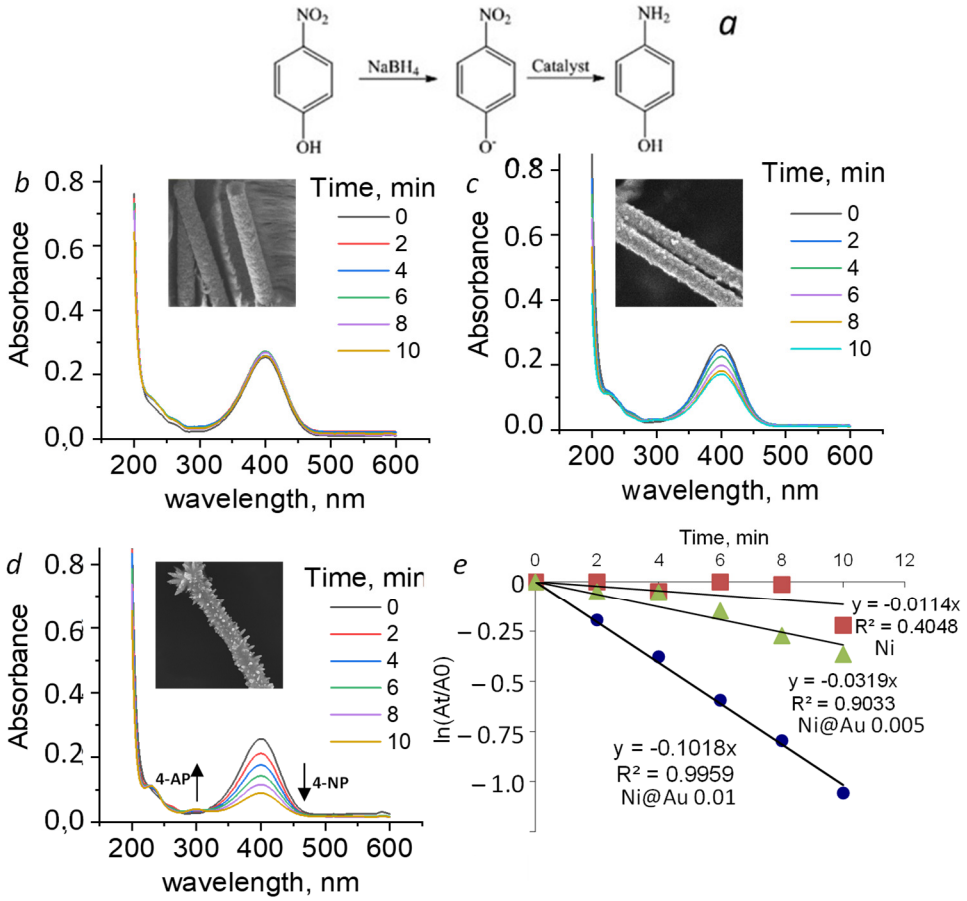

Figure 6. Catalytic reaction of the reduction of 4-nitrophenol by borohydride ions in an aqueous solution (**a**). UV-FTIR spectra of the reduction in the presence of Ni (**b**), Ni@Au 0.005 M (**c**), and Ni@Au 0.01 M (**d**). Kinetic analysis of the competitive reduction according to Equation (6) (**e**).

The reaction was tested in five cycles (runs), and the change in the reaction efficiency is shown in Figure 7. We observed at first a slight decrease in the efficiency of 78 and 65%, compared with the first run; however, after the fifth cycle, the reaction efficiency dropped to 48%, which could be due to a decrease in the amount of recovered material with the use of a magnet.

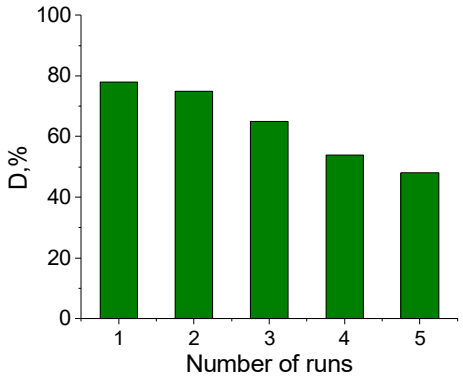

Figure 7. Efficiency of Ni@Au 0.01 M in 5 sequential cycles of reduction of 4-nitrophenol.

4. Conclusions

We have shown that Ni nanotubes (NTs) produced by a convenient template synthesis are suitable for deposition of nanostructured gold directly on their surface using a solution of tetrachloroauric acid. By varying the concentration of gold salts in the initial solution, a layer of pure gold of two different morphologies was obtained on nickel NTs: a uniform layer of smooth nanoparticles and a layer with nano-needles. The proposed method of Ni nanotubes surface modification very slightly affects the magnetic properties of Ni NTs, since few changes were observed in the structure of the magnetic core. A significant catalytic activity of Ni@Au NTs was demonstrated using a model reaction of reduction of 4-nitrophenol. The efficiency depended on the state of the Au surface of such structures. The largest value of the reaction rate of 1.7×10^{-3} s^{-1} was obtained in the presence of Ni@Au NTs (0.01 M) with Au layer having nano-needles. The presence of the magnetic support allowed the catalysts' removal with a magnet for reuse.

Author Contributions: Conceptualization: A.R., A.K. and E.K.; methodology, A.S.; validation, Z.I., I.K. and M.Z.; investigation, Z.I., I.K. and M.Z.; resources, L.P.; writing—original draft preparation, A.S.; writing—review and editing, L.P.; funding acquisition, L.P. All authors have read and agreed to the published version of the manuscript.

Funding: The work was carried out with the support of the Ministry of Science and Higher Education of the Russian Federation in the framework of the State Task (project code 0718-2020-0037).

Institutional Review Board Statement: Not applicable.

Conflicts of Interest: The authors declare no conflict of interest.

References

1. Amendola, V.; Pilot, R.; Frasconi, M.; Maragò, O.M.; Iatì, M.A. Surface plasmon resonance in gold nanoparticles: A review. *J. Phys. Condens. Matter.* **2017**, *29*, 203002. [CrossRef] [PubMed]
2. Daniel, M.-C.; Astruc, D. Gold Nanoparticles: Assembly, Supramolecular Chemistry, Quantum-Size-Related Properties, and Applications toward Biology, Catalysis, and Nanotechnology. *Chem. Rev.* **2004**, *104*, 293–346. [CrossRef]
3. Campbell, C.T. The active site in nanoparticle gold catalysis. *Science* **2004**, *306*, 234–235. [CrossRef]
4. Son, H.Y.; Kim, K.R.; Hong, C.A.; Nam, Y.S. Morphological evolution of gold nanoparticles into nanodendrites using catechol-grafted polymer templates. *ACS Omega* **2018**, *3*, 6683–6691. [CrossRef]
5. Haruta, M. Size- and support-dependency in the catalysis of gold. *Catal. Today* **1997**, *36*, 153–166. [CrossRef]
6. Lin, C.; Tao, K.; Hua, D.; Ma, Z.; Zhou, S. Size effect of gold nanoparticles in catalytic reduction of p-nitrophenol with $NaBH_4$. *Molecules* **2013**, *18*, 12609–12620. [CrossRef]
7. Somorjai, G.A.; Li, Y. *Introduction to Surface Chemistry and Catalysis*; Wiley: Hoboken, NJ, USA, 2010.

8. Alam, M.N.; Batuta, S.; Ahamed, G.; Das, S.; Mandal, D.; Begum, N.A. Tailoring the catalytic activity of Au nanoparticles synthesized by a naturally occurring green multifunctional agent. *Arab. J. Chem.* **2019**, *12*, 3825–3835. [CrossRef]
9. Wang, D.; Sun, Y.; Huang, J.; Liang, Z.; Li, S.; Jiang, L. Morphological effects on the selectivity of intramolecular: Versus intermolecular catalytic reaction on Au nanoparticles. *Nanoscale* **2017**, *9*, 7727–7733. [CrossRef]
10. Wu, B.; Kuang, Y.; Zhang, X.; Chen, J. Noble metal nanoparticles/carbon nanotubes nanohybrids: Synthesis and applications. *Nano Today* **2011**, *6*, 75–90. [CrossRef]
11. Alshammari, H.M.; Alshammari, A.S.; Humaidi, J.R.; Alzahrani, S.A.; Alhumaimess, M.S.; Aldosari, O.F.; Hassan, H.M.A. Au-Pd bimetallic nanocatalysts incorporated into carbon nanotubes (CNTs) for selective oxidation of alkenes and alcohol. *Processes* **2020**, *8*, 1380. [CrossRef]
12. Kazemi, M. Based on magnetic nanoparticles: Gold reusable nanomagnetic catalysts in organic synthesis. *Synth. Commun.* **2020**, *50*, 2079–2094. [CrossRef]
13. Zhao, P.; Feng, X.; Huang, D.; Yang, G.; Astruc, D. Basic concepts and recent advances in nitrophenol reduction by gold- and other transition metal nanoparticles. *Coord. Chem. Rev.* **2015**, *287*, 114–136. [CrossRef]
14. Mitchell, D.T.; Lee, S.B.; Trofin, L.; Li, N.; Nevanen, T.K.; Soderland, H.; Martin, C.R. Smart Nanotubes for Bioseparations and Biocatalysis. *J. Am. Chem. Soc.* **2002**, *124*, 11864–11865. [CrossRef]
15. Mashentseva, A.A.; Shlimas, D.I.; Kozlovskiy, A.L.; Zdorovets, M.V.; Russakova, A.V.; Kassymzhanov, M.; Borisenko, A.N. Electron Beam Induced Enhancement of the Catalytic Properties of Ion-Track Membranes Supported Copper Nanotubes in the Reaction of the P-Nitrophenol Reduction. *Catalysts* **2019**, *9*, 737. [CrossRef]
16. Zhang, W.; Tan, F.; Wang, W.; Qiu, X.; Qiao, X.; Chen, J. Facile, template-free synthesis of silver nanodendrites with high catalytic activity for the reduction of p-nitrophenol. *J. Hazard. Mater.* **2012**, *217–218*, 36–42. [CrossRef] [PubMed]
17. Alshammari, H.M.; Humaidi, J.R.; Alhumaimess, M.S.; Aldosari, O.F.; Alotaibi, M.H.; Hassan, H.M.A.; Wawata, I. Bimetallic Au:Pd nanoparticle supported on MgO for the oxidation of benzyl alcohol. *Reac. Kinet. Mech. Cat.* **2019**, *128*, 97–108. [CrossRef]
18. Thongthai, K.; Srisombat, L.; Saipanya, S.; Ananta, S. Morphology and atalytic activity of gold core-platinum shell nanoparticles. *Chiang Mai J. Sci.* **2015**, *42*, 481–489.
19. Roselina, N.R.; Azizan, A.; Hyie, K.M.; Murad, M.C.; Abdullah, A.H. Synthesis and characterization of Ni-Au bimetallic nanoparticles. *Int. J. Mod. Phys. B* **2015**, *29*, 1540006. [CrossRef]
20. Ahmad, T.; Bae, H.; Rhee, I.; Chang, Y.; Jin, S.-U.; Hong, S. Gold-coated iron oxide nanoparticles as a contrast agent in magnetic resonance imaging. *J. Nanosci. Nanotechnol.* **2012**, *12*, 5132–5137. [CrossRef] [PubMed]
21. Silva, S.M.; Tavallaie, R.; Sandiford, L.; Tilley, R.D.; Gooding, J.J. Gold coated magnetic nanoparticles: From preparation to surface modification for analytical and biomedical applications. *Chem. Commun.* **2016**, *52*, 7528–7540. [CrossRef]
22. Kozlovskiy, A.; Zdorovets, M.; Shumskaya, A.; Kanyukov, E.; Kutuzau, M. Synthesis and Properties of Ni x/Au 1-x Nanotubes. In Proceedings of the 2017 IEEE 7th International Conference Nanomaterials: Application & Properties (NAP), Odessa, Ukraine, 10–15 September 2017; pp. 04NB21-1–04NB21-3.
23. Korolkov, I.V.; Mashentseva, A.A.; Güven, O.; Gorin, Y.G.; Kozlovskiy, A.L.; Zdorovets, M.V.; Zhidkov, I.S.; Cholach, S.O. Electron/gamma radiation-induced synthesis and catalytic activity of gold nanoparticles supported on track-etched poly(ethylene terephthalate) membranes. *Mater. Chem. Phys.* **2018**, *217*, 31–39. [CrossRef]
24. Mashentseva, A.A.; Ibragimova, M.A.; Akhmetova, S.B.; Kozlovskiy, A.L. Synthesis, radical scavenging, and antimicrobial activities of core–shell Au / Ni microtubes. *Chem. Pap.* **2020**, *74*, 2189–2199. [CrossRef]
25. Shokouhimehr, M. Magnetically separable and sustainable nanostructured catalysts for heterogeneous reduction of nitroaromatics. *Catalysts.* **2015**, *5*, 534–560. [CrossRef]
26. Pondman, K.M.; Maijenburg, A.W.; Celikkol, F.B.; Pathan, A.A.; Kishore, U.; ten Haken, B.; ten Elshof, J.E. Au coated Ni nanowires with tuneable dimensions for biomedical applications. *J. Mater. Chem. B* **2013**, *1*, 6129–6136. [CrossRef]
27. Wu, Z.; Zhao, Z.; Zhang, M. Synthesis by Replacement Reaction and Application of TiO_2-Supported Au-Ni Bimetallic Catalyst. *ChemCatChem* **2010**, *2*, 1606–1614. [CrossRef]
28. Cárdenas-Lizana, F.; Keane, M.A. Gas phase selective hydrogenation over oxide supported Ni-Au. *Phys. Chem. Chem. Phys.* **2015**, *17*, 28088–28095. [CrossRef] [PubMed]
29. Ruppert, A.M.; Jędrzejczyk, M.; Potrzebowska, N.; Kaźmierczak, K.; Brzezińska, M.; Sneka-Płatek, O.; Sautet, P.; Keller, N.; Michel, C.; Grams, J. Supported gold-nickel nano-alloy as a highly efficient catalyst in levulinic acid hydrogenation with formic acid as an internal hydrogen source. *Catal. Sci. Technol.* **2018**, *8*, 4318–4331. [CrossRef]
30. Wang, F.; Yang, X.; Zhang, J. Well-dispersed $MgAl_2O_4$ supported Ni catalyst with enhanced catalytic performance and the reason of its deactivation for long-term dry methanation reaction. *Catalysts* **2021**, *11*, 1117. [CrossRef]
31. Chin, Y.H.; King, D.L.; Roh, H.S.; Wang, Y.; Heald, S.M. Structure and reactivity investigations on supported bimetallic Au{single bond}Ni catalysts used for hydrocarbon steam reforming. *J. Catal.* **2006**, *244*, 153–162. [CrossRef]
32. Kaniukov, E.Y.; Shumskaya, E.E.; Yakimchuk, D.V.; Kozlovskiy, A.L.; Ibragimova, M.A.; Zdorovets, M.V. Evolution of the polyethylene terephthalate track membranes parameters at the etching process. *J. Contem. Phys.* **2017**, *52*, 155–160. [CrossRef]
33. Kozlovskiy, A.; Borgekov, K.; Zdorovets, M.; Arkhangelsky, E.; Shumskaya, A.; Kanukov, E. Application of ion-track membranes in processes of direct and reverse osmosis. *Proc. Natl. Acad. Sci. Belarus* **2017**, *1*, 45–51.
34. Korolkov, I.V.; Mashentseva, A.A.; Güven, O.; Zdorovets, M.V.; Taltenov, A.A. Enhancing hydrophilicity and water permeability of PET track-etched membranes by advanced oxidation process. *Nucl. Instrum. Meth. Phys. Res. B* **2015**, *365*, 651–655. [CrossRef]

35. Korolkov, I.V.; Güven, O.; Mashentseva, A.A.; Atıcı, A.B.; Gorin, Y.G.; Zdorovets, M.V.; Taltenov, A.A. Radiation induced deposition of copper nanoparticles inside the nanochannels of poly(acrylic acid)-grafted poly(ethylene terephthalate) track-etched membranes. *Radiat. Phys. Chem.* **2017**, *130*, 480–487. [CrossRef]
36. Kaniukov, E.; Kozlovsky, A.; Shlimas, D.; Yakimchuk, D.; Zdorovets, M.; Kadyrzhanov, K. Tunable synthesis of copper nanotubes. *IOP Conf. Ser. Mater. Sci. Eng.* **2016**, *110*, 012013. [CrossRef]
37. Kalkabay, G.; Kozlovskiy, A.; Zdorovets, M.; Borgekov, D.; Kaniukov, E.; Shumskaya, A. Influence of temperature and electrodeposition potential on structure and magnetic properties of nickel nanotubes. *J. Magn. Magn. Mater.* **2019**, *489*, 165436. [CrossRef]
38. Shumskaya, A.; Bundyukova, V.; Kozlovskiy, A.; Zdorovets, M.; Kadyrzhanov, K.; Kalkabay, G.; Kaniukov, E. Evolution of morphology, structure, and magnetic parameters of Ni nanotubes with growth in pores of a PET template. *J. Magn. Magn. Mater.* **2020**, *497*, 165913. [CrossRef]
39. Shumskaya, A.; Korolkov, I.; Rogachev, A.; Ignatovich, Zh.; Kozlovskiy, A.; Zdorovets, M.; Anisovich, M.; Bashouti, M.; Shalabny, A.; Busool, R.; et al. Synthesis of Ni@Au core-shell magnetic nanotubes for bioapplication and SERS detection. *Colloids Surf. A Physicochem. Eng.* **2021**, *626*, 127077. [CrossRef]
40. Korolkov, I.V.; Ludzik, K.; Kozlovskiy, A.L.; Fadeev, M.S.; Shumskaya, A.E.; Gorin, Y.G.; Marciniak, B.; Jazdzewska, M.; Chudoba, D.; Kontek, R.; et al. Carboranes immobilization on Fe3O4 nanocomposites for targeted delivery. *Mater. Today Commun.* **2020**, *24*, 101247. [CrossRef]
41. Ciganda, R.; Li, N.; Deraedt, C.; Gatard, S.; Zhao, P. Gold nanoparticles as electron reservoir redox catalysts for 4-nitrophenol reduction: A strong stereoelectronic ligand influence. *ChemComm.* **2014**, *50*, 10126–10129. [CrossRef]
42. Kuroda, K.; Ishida, T.; Haruta, M. Reduction of 4-nitrophenol to 4-aminophenol over Au nanoparticles deposited on PMMA. *J. Mol. Catal. A Chem.* **2009**, *298*, 7–11. [CrossRef]